ADVANCED FUNCTIONAL MATERIALS
www.afm-journal.de

www.MaterialsViews.com

Sodium and Potassium Ion Selective Conjugated Polymers for Optical Ion Detection in Solution and Solid State

Alexander Giovannitti, Christian B. Nielsen, Jonathan Rivnay, Mindaugas Kirkus, David J. Harkin, Andrew J.P. White, Henning Sirringhaus, George G. Malliaras, and Iain McCulloch*

This paper presents the development of alkali metal ion selective small molecules and conjugated polymers for optical ion sensing. A crown ether bithiophene unit is chosen as the detecting unit, as both a small molecule and incorporated into a conjugated aromatic structure. The complex formation and the resulting backbone twist of the detector unit is investigated by UV–vis and NMR spectroscopy where a remarkable selectivity toward sodium or potassium ions is found. X-ray diffraction analysis of single crystals with and without alkali metal ions is carried out and a difference of the dihedral angle of more than 70° is observed. In a conjugated polymer structure, the detector unit has a higher sensitivity for alkali metal ion detection than its small molecule analog. Ion selectivity is retained in polymers with solubility in polar solvents facilitated by the attachment of polar ethylene glycol side chains. This design concept is further evolved to develop a sodium-salt solid state sensor based on blends of the detecting polymer with a polyvinyl alcohol matrix where the detection of sodium ions is achieved in aqueous salt solutions with concentrations similar to biologically important environments.

1. Introduction

Ion selective conjugated polymers are excellent materials for the fabrication of optical sensors in solution and solid state. The synthetic freedom for designing polymers with ion selectivity and solution processability makes these materials highly interesting for optical sensors. The working principle of previously reported alkali metal salt selective optical sensors is usually based on ion exchange membranes which can be triggered by changing the pH.[1,2] The disadvantage is that they normally consist of several components, while the sensor material is usually a protonated cation selective dye which forms a complex with the salt under acid conditions.[3–5] The most efficient way to create ion selectivity for alkali metal ions in pH neutral solutions is by using crown ether molecules.[6] The size of the crown ether ring and the alkali metal ion determine the stability of the complex. For example, ion selective membranes comprising crown ethers allow concentration-dependent potentiometric measurements of sodium and potassium ions in blood fluids.[7–9] An optical sensor based on crown ethers has the advantage of rapid and selective sensing when the crown ether is attached to a conjugated π-electron system which absorbs and/or emits in the visible light spectrum.[10] Crown ethers attached in the third and fourth positions of thiophene show selectivity toward sodium ions in both small molecules[11] and polymers.[12] Variation in the heteroatoms of the crown ether demonstrated the ability for complexation of various ions, such as Pb^{2+},[13] Ag^{+}, and Hg^{2+}.[14] An approach based on a crown ether attached in the 3- and 3′-positions of 2,2′-bithiophene was demonstrated, where a conformational change induced by alkali metal ions was postulated and an ion selective response with alkali metal ions was reported.[15] This approach was subsequently used as a switchable molecular wire triggered by sodium salts.[16] The development of sensors for sensitive and dynamic monitoring of ions is critical for environmental and health monitoring. The concentration of cations such as sodium and potassium is important for electrolyte balance in extracellular and intracellular fluids and is especially vital to the activity of nerve and muscle cells. Detection of deviations in their concentrations is typical in health monitoring and early disease diagnosis.

In this work we present the development and characterization of visible sensor materials for highly selective sodium- and potassium-salt detection in solution and solid state, based

A. Giovannitti, Dr. C. B. Nielsen, Dr. M. Kirkus, Dr. A. J. P. White, Prof. I. McCulloch
Department of Chemistry
and Centre for Plastic Electronics
Imperial College London
London SW7 2AZ, UK
E-mail: A.Giovannitti13@imperial.ac.uk
Dr. J. Rivnay,[+] Prof. G. G. Malliaras
Department of Bioelectronics
École Nationale Supérieure des Mines
CMP-EMSE, MOC, Gardanne 13541, France
D. J. Harkin, Prof. H. Sirringhaus
Department of Physics
University of Cambridge
Cambridge CB3 0HE, UK
[+]Present address: Palo Alto Research Center, Palo Alto, CA 94304, USA

This is an open access article under the terms of the Creative Commons Attribution License, which permits use, distribution and reproduction in any medium, provided the original work is properly cited.

DOI: 10.1002/adfm.201503791

© 2015 The Authors. Published by WILEY-VCH Verlag GmbH & Co. KGaA, Weinheim

on conjugated aromatic crown ether bithiophene materials. Crown ether bithiophene small molecules and copolymers with benzo[1,2-*b*:4,5-*b'*]dithiophene (BDT) were synthesized and a detailed structural characterization of the complex formation with different alkali metal salts was performed. Selectivity toward sodium or potassium ions was observed for different crown ether ring sizes of the small molecules with the excellent selectivity retained in the corresponding polymers. Next to a blue shift of the absorption maximum, a shift of the emission peak to higher energy was also observed when alkali metal ions were added. We also present the development of an optical sodium ion solid state sensor working in aqueous solution utilizing the crown ether copolymers comprising highly polar side chains in a blend with polyvinyl alcohol (PVA). The formation of hydrogel morphology allows efficient ion penetration into the bulk conjugated polymer.

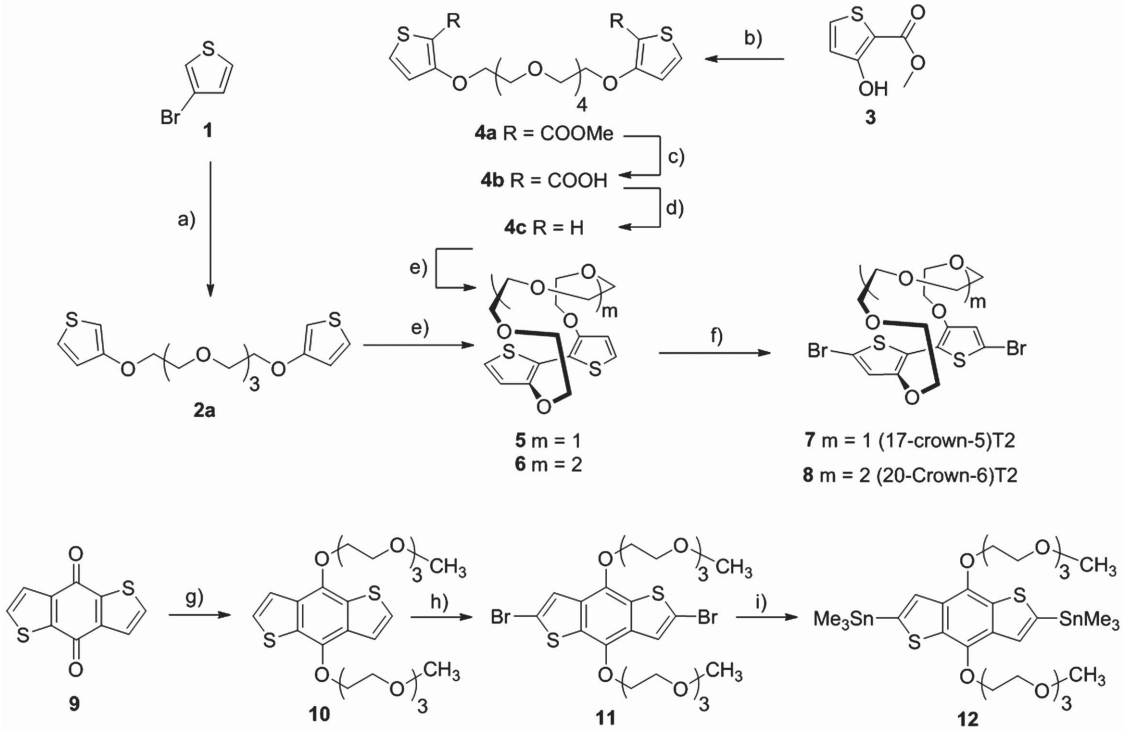
2. Results and Discussion

2.1. Synthesis and Characterization

The synthesis of the dibrominated crown ether functionalized bithiophene small molecules (17-Crown-5)T2 and (20-Crown-6) T2 is shown in **Scheme 1**. For both small molecules the thiophene-flanked glycol intermediates **2a** and **4c** were synthesized. A reaction screening for the intermediate 2a was carried out to increase the yield of the alkoxylation of 3-bromothiophene (Scheme 1, step a) and it was found that CuI as the catalyst and a catalyst loading of 15 mol% in *N,N*-dimethylformamide (DMF) achieved the highest yield (41%, compared to 32.5% lit.[15]). A variation in the reaction route was chosen for the intermediate **4c** (Scheme 1, steps b–d) based on the literature[17] which improved the yield of **4c** to 61% (compared to 36% lit.[15]) and avoided the air-sensitive copper(I)-mediated alkoxylation. A selective ring closure in the two positions of the thiophenes[15] afforded the head-to-head-coupled alkoxy-bithiophenes **5** and **6** in Scheme 1. The electron-rich bithiophene units were subsequently brominated with *N*-bromosuccinimide (NBS) at –20 °C. The synthesis of (4,8-bis(triethylene glycol(TEG))benzo[1,2-b:4,5-b']dithiophene-2,6-diyl)bis(trimethylstannane) **12** is presented in Scheme 1 The formation of the BDT unit with methyl-endcapped triethylene glycol side chains **10** was achieved by following a literature procedure.[18] The bromination was only possible under alkaline conditions with *n*-BuLi and CBr_4 while the bromination under acidic conditions with NBS reversed the first reaction in Scheme 1 and the starting material **9** was mainly isolated. It was necessary to prepare the distannylated monomer **12** in high purity in order to facilitate polymerization. It was found that only the halogen–metal exchange of **11** at –78 °C with an excess of five equivalents *n*-BuLi in THF over 3 h achieved full conversion to the desired distannylated product **12**.

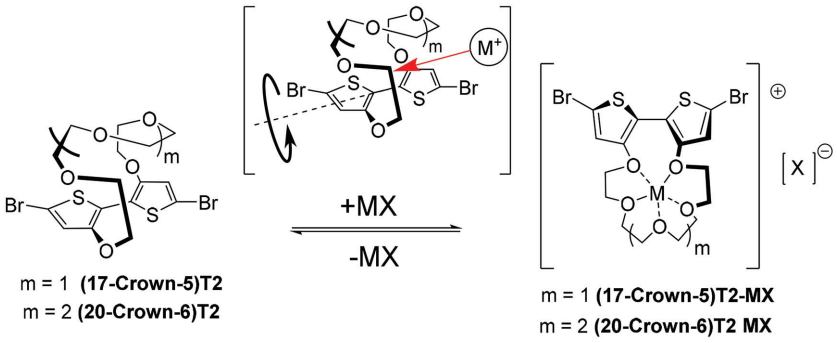
2.2. Characterization of the Backbone Twist

Scheme 2 shows an illustration of the formation of the complex between the synthesized small molecules (17-Crown-5)T2,



Scheme 1. Synthesis of molecules **7**, **8** and **12**. Conditions: a) tetraethylene glycol, NaH, CuI, DMF [42%] (**2a**), b) $TsO(CH_2CH_2O)_5$ Ts, K_2CO_3, DMF, [95%] (**4a**), c) KOH, H_2O:EtOH, [98%] (**4b**), d) Cu_2O, pyridine, [65%] (**4c**), e) *m* = 1: *n*-BuLi, $CuCl_2$, DME [18 %] (**5**), *m* = 2: *n*-BuLi, $CuCl_2$, DME [25%] (**6**), f) *m* = 1: NBS, $CHCl_3$ [47%] (**7**), *m* = 2: NBS, $CHCl_3$ [54%] (**8**), g) Zn, NaOH, $TsO(CH_2CH_2O)_3Me$, EtOH:H_2O (5:1) [41%] (**10**), h) *n*-BuLi, LiCl, CBr_4,THF [39%] (**11**), i) *n*-BuLi, Me_3SnCl, THF [23%] (**12**).

© 2015 The Authors. Published by WILEY-VCH Verlag GmbH & Co. KGaA, Weinheim



Scheme 2. Formation of the complexes and the resulting backbone twist.

(20-Crown-6)T2 and alkali metal salts MX (M = Na, K; X = ClO_4, BPh_4). The formation of complexes (17-Crown-5)T2-MX and (20-Crown-6)T2-MX requires a twist of the bithiophene unit to form a conformer where the two oxygen atoms attached to the thiophenes are in close proximity with each other.

This conformational twist was monitored by UV-vis and NMR spectroscopy as well as X-ray diffraction of single crystals with and without alkali metal salts to investigate the change of the dihedral angle of the fused thiophene rings in solution and in the solid state. In particular, the concentration of the alkali metal salts in solution was varied to analyze selectivity and sensitivity of the small molecules. The selectivity of the small molecules toward alkali metal ions was studied by UV-vis spectroscopy titration experiments where the absorption was monitored as a function of the concentration of MX. **Figure 1** shows the complexation reaction and the optical responses of the small molecules in acetonitrile at 25 °C when the concentration of $MClO_4$ (M = Na, K) was increased incrementally. A blue shift of 40 nm of the absorption maximum was observed when (17-Crown-5)T2 was treated with $NaClO_4$ with an isosbestic point at 310 nm (Figure 1a), while no changes of the optical properties were observed when lithium or potassium perchlorates were added (Figure 1c), (series of all salts, Supporting Information). On the other hand, it was found that the larger molecule (20-Crown-6)T2 exclusively forms the twisted complex structure with potassium salts (Figure 1b), and a corresponding 50 nm blue shift of the absorption maximum

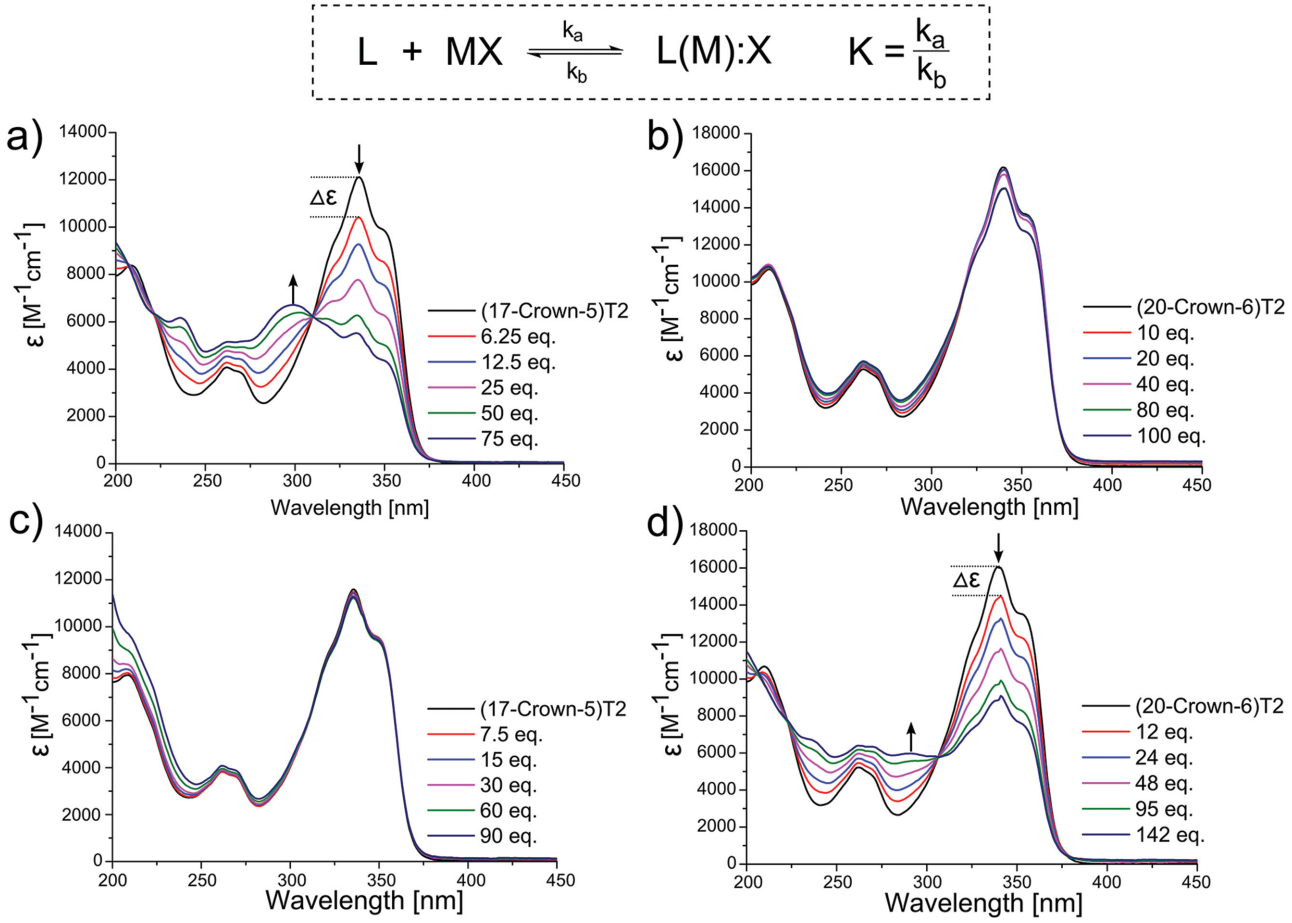


Figure 1. Complex formation and stability complex constant (ligand L is the small molecule, MX is the salt, and L(M):X represents the formed complex). UV–vis spectroscopy titration experiments of (17-Crown-5)T2 and (20-Crown–6)T2 with $NaClO_4$ (a,b) and (17-Crown–5)T2 and (20-Crown-6)T2 with $KClO_4$ (c,d) in acetonitrile at 25 °C.

© 2015 The Authors. Published by WILEY-VCH Verlag GmbH & Co. KGaA, Weinheim

Table 1. Stability complex constants for the sodium and potassium complexes in acetonitrile at 25 °C.

Ligand	log *K* ($NaClO_4$) [L mol^{-1}]	log *K* ($KClO_4$) [L mol^{-1}]	$\Delta\varepsilon$ [(M^{-1} cm^{-1})][d]
17-(Crown-5)T2	2.58[a]	–	4383
20-(Crown-6)T2	–	2.41[a]	3279
15-Crown-5[19]	4.44[b]	3.38[b]	–
18-Crown-6[20]	4.21[c]	5.46[c]	–

[a]Calculated from UV–vis data; [b]conductivity measurements;[19] [c]NMR measurements;[20] [d]after addition of 50 equivalents of $MClO_4$.

was observed with an isosbestic point at 306 nm. The extinction coefficients of the functionalized bithiophenes substantially decreased (41% for (17-Crown-5)T2 and 22% for (20-Crown-6)T2 after 50 equivalents $MBPh_4$, **Table 1**) when the twisted complexes were formed. This can be explained by a conformation change resulting in a lower transition dipole moment of the twisted structure compared to the planar structure, due to reduced molecular orbital overlap.

The stability constants for the sodium and potassium salt complexes were derived from the UV–vis data (Supporting Information) and are listed in Table 1. We compare them to 1,4,7,10,13-pentaoxacyclopentadecane (15-Crown-5) and 1,4,7,10,13,16-hexaoxacyclooctadecane (18-Crown-6) which have high complexation tendencies for sodium and potassium salts, respectively. As shown in Table 1, 15-Crown-5 and 18-Crown-6 form highly stable complexes with sodium and/or potassium salts which limit the usage of these materials for highly selective measurements. The complex stability constants are very high which limits the long term usage due to a lack of reversibility of the complexation for these materials. For our synthesized materials the optical selectivity for either sodium salts (17-Crown-5)T2 or potassium salts (20-Crown-6)T2 is remarkable and makes the materials highly interesting for optical sensors. It was found that the sodium complex with (17-Crown-5)T2 has a slightly higher stability than the potassium complex with (20-Crown-6)T2.

The stability constants are lower than their respective crown ether analogs due to the electronic nature where the twist of the thiophenes forms a conformation with a higher energy as a result of a decreased conjugation length of the aromatic system. Another reason could be a side complexation reaction where the metal ion is stabilized by the crown ether but the structure does not undergo a backbone twist.[21,22]

To get a better understanding of the side complexation reaction, a detailed NMR spectroscopy study was carried out with (17-Crown-5)T2 and (20-Crown-6)T2 and different alkali metal salts MX. The structure of the small molecule (17-Crown-5)T2 is shown in **Figure 2**a where the crown ether protons (A–D) as well as the aromatic protons (E) are labeled. Protons A nearest to the electron-rich aromatic system are highly deshielded and have a chemical shift at higher frequencies (4.3 ppm) while protons C and D are shielded (3.37 and 3.26 ppm) but surprisingly resolved. This unexpected resolution of the signals indicates a planarized structure of (17-Crown-5)T2 in solution which can be explained by sulfur oxygen interactions of the bithiophene unit.[23] Temperature-dependent ^{1}H NMR measurements were carried out to investigate a conformational change from a planar to a twisted structure at higher temperature. It was found that a temperature difference of 50 °C shifted protons B, C, and D to higher frequencies while proton A was unaffected. This shift of the protons B, C, and D indicates a change of the conformation (Supporting Information). Figure 2b shows the response of the crown ether protons of (17-Crown-5)T2 when the concentration of $NaBPh_4$ was increased in deuterated acetonitrile. Before the addition, all crown ether protons of (17-Crown-5)T2 are highly resolved (labeled A, B, C, and D in Figure 2a). The resolved signals and shift toward lower frequencies of protons C and D are further evidence for a planar structure because the protons are located above the aromatic system and the induced magnetic field of the aromatic system shields the protons. During the salt addition, the chemical shift of proton A shifts toward lower frequencies which is consistent with a decrease of electron density due to the charge transfer from the oxygen atoms to the metal ion. Surprisingly, we observed a shift to higher frequencies for protons C and D when the salt concentration was increased and the signals become less resolved while at high salt concentrations the signals even merge together where both protons have the same chemical environment. As illustrated in **Figure 3**a, the protons C and D are only located above the aromatic system in a planar structure while the aromatic ring current of the twisted aromatic bithiophene structure does not affect the protons (Figure 3b).

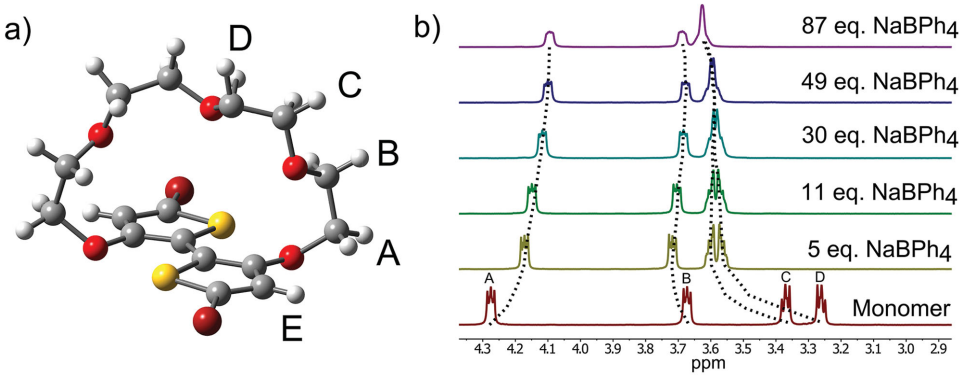


Figure 2. a) Molecular structure of (17-Crown-5)T2 with labeled hydrogen atoms A–E, b) titration experiment analyzed by NMR spectroscopy, crown ether protons of (17-Crown-5)T2 in the region of 4.3–2.9 ppm in acetonitrile-d_3 and addition of up to 87 equivalents of $NaBPh_4$. All spectra are referenced to acetonitrile-d_3 and protons A–D are highlighted.

© 2015 The Authors. Published by WILEY-VCH Verlag GmbH & Co. KGaA, Weinheim

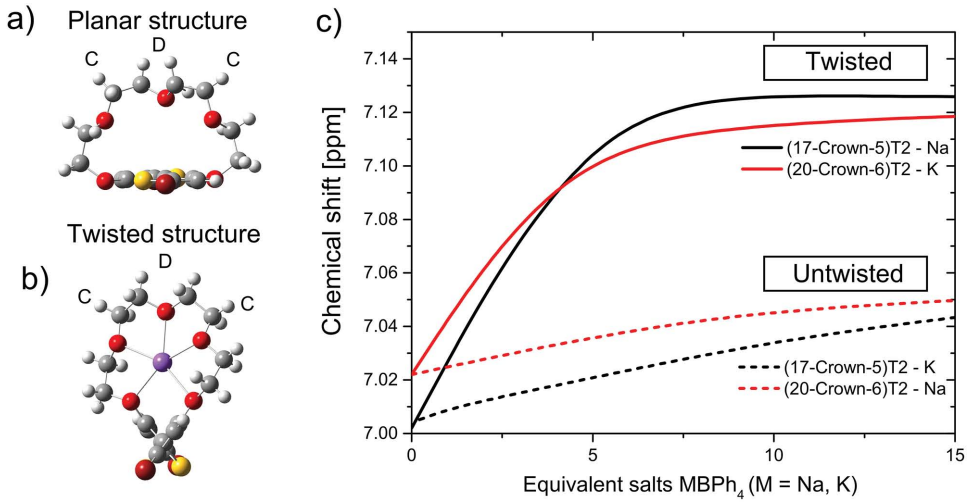


Figure 3. a) Planar structure of (17-Crown-5)T2: Protons C and D are above the aromatic system. b) Twisted structure: protons are less affected by the aromatic system. c) Change of the chemical shift of protons E when the twisted or an untwisted complex is formed in acetonitirle-d_3.

The response of the small molecules (17-Crown-5)T2 and (20-Crown-6)T2 toward sodium and potassium salts (salt comparison, Supporting Information) was measured by NMR spectroscopy and compared to each other. It was found that the crown ether protons of (17-Crown-5)T2 only shifted strongly when sodium salt was added while a minor shift was found for the potassium salt. The crown ether protons of (20-Crown-6)T2 interacted with both sodium and potassium salts which is due to the slightly larger crown ether which allows the complex formation with sodium and potassium salts also when the small molecule (20-Crown-6)T2 do not form the twisted complex structure as described above.[20] Our finding that the crown ether units also interact with the added salts without forming the twisted complexes provides another explanation for the low complex stability constants. However, a significant difference in the chemical shifts of the aromatic protons E was found when the salt was added which form the twisted complex. As shown in Figure 3c, the signals of the aromatic protons E shifted 0.10 ppm (17-Crown-5)T2 and 0.12 ppm (20-Crown-6)T2 when the twisted complexes were formed, while the shifts of the signals of the untwisted complex were only 0.041 and 0.036 ppm after addition of 15 equivalents of salts. This shows that the aromatic protons E are highly affected by the formation of the twisted structure and this also proves that the interaction of (20-Crown-6)T2 with $NaBPh_4$ does not form the twisted complex structure and only interacts with the crown ether protons. Nuclear overhauser effect (NOE) experiments for (17-Crown-5)T2 are another evidence for a change of the conformation (Supporting Information).

Single crystal X-ray diffraction analyses were carried out to investigate the molecular structures of the crown ethers and their alkali metal salt complexes. **Figure 4** shows the molecular crystal structures of (17-Crown-5)T2 and (20-Crown-6)T2 with and without alkali metal salts. A dihedral angle of 3.2° for (17-Crown-5)T2 was observed while the angle increases to 75.9° when the $NaBPh_4$ complex is formed. The dihedral angle of (20-Crown-6)T2 increases from 14.0° to 84.6° when the complex with $KClO_4$ is formed.

2.3. Polymerization

The high selectivity of the small molecule (17-Crown-5)T2 toward sodium and of (20-Crown-6)T2 toward potassium encouraged us to synthesize a series of polymers incorporating the ion selective monomers in the backbone, to investigate sodium- and potassium-selective sensor materials. Two different types of distannylated BDTmonomers were prepared containing either 5-ethylhexyl-2-thienyl[24] or TEG side chains. The alkylated BDT monomer was prepared in order to use the common conditions for Stille polymerization and allow processing from nonpolar solvents. The triethylene glycol BDT unit was synthesized to achieve solubility in polar solvents, which will allow processing from polar solvents, e.g., DMF or acetonitrile. Alternating copolymers were synthesized by Pd-catalyzed Stille polymerization in chlorobenzene as illustrated in **Scheme 3**.[25] We copolymerized the dibrominated small molecules (17-Crown-5)T2 and (20-Crown-6)T2 with the distannylated BDT monomers[26] to afford polymers **P1** and **P2** with 5-ethylhexyl-2-thienyl side chains and polymers **P3** and **P4** with triethylene glycol side chains. Polymers **P1** and **P2** were obtained with respectable molecular weights (M_n = 26 kDa, M_w = 73 kDa for **P1**, M_n = 30 kDa, M_w = 44 kDa for **P2**) whereas lower molecular weights were obtained for polymers **P3** and **P4** (M_n = 3.2 kDa, M_w = 5.6 kDa for **P3**, M_n = 3.6 kDa, M_w = 6.0 kDa for **P4**). Matrix-assisted laser desorption/ionization–time-of-flight (MALDI–TOF) mass spectrometry of **P3** and **P4** showed several repeating units (Supporting Information) indicating the successful incorporation of the crown ether units in the structure.

2.4. Optoelectronic Properties

The UV–vis titration experiments of polymer **P1** and alkali metal salts $MBPh_4$ (M = Na, K) in tetrahydrofuran (THF) are shown in **Figure 5**. A blue shift of 75 nm of the absorption maximum was observed when $NaBPh_4$ was added (Figure 5a).

© 2015 The Authors. Published by WILEY-VCH Verlag GmbH & Co. KGaA, Weinheim

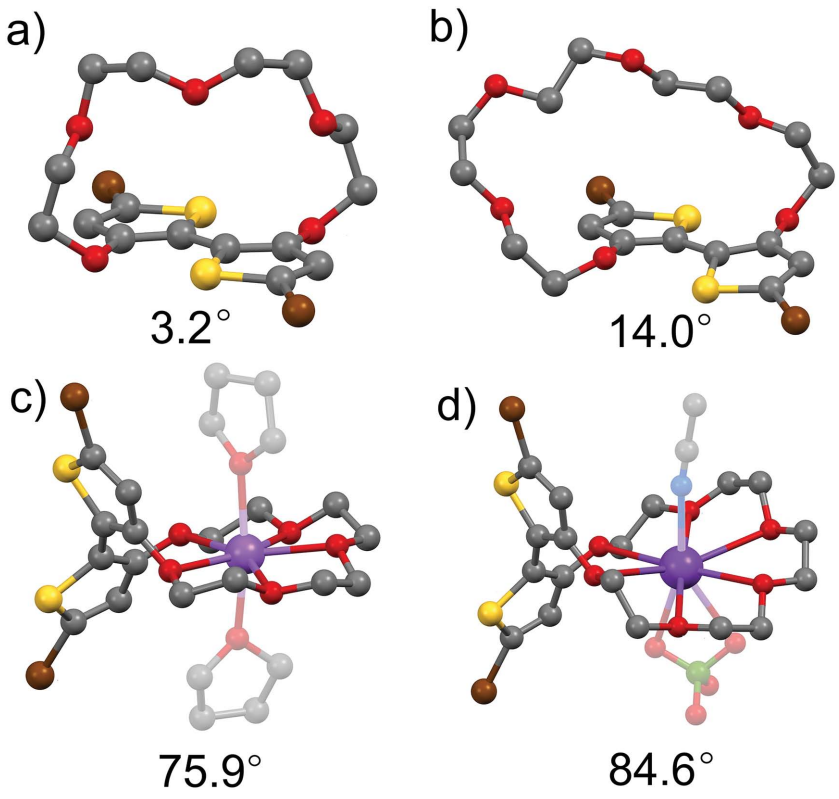


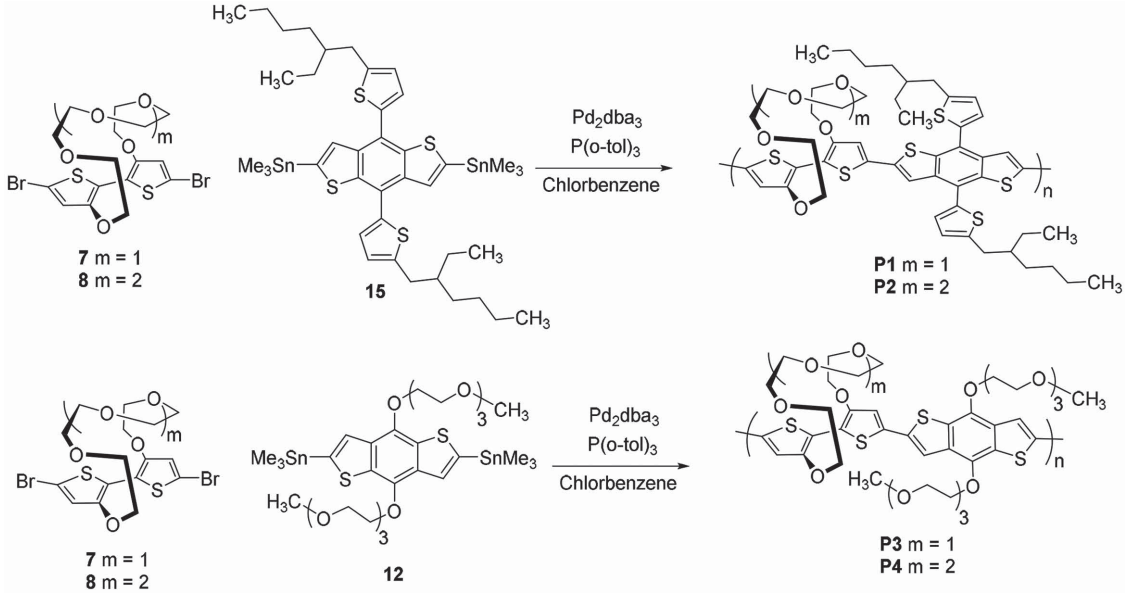
Figure 4. a) Crystal structure of (17-Crown-5)T2. b) Crystal structure (20-Crown-6)T2. c) Crystal structure of complex (17-Crown-5)T2:$NaBPh_4$ stabilized by two THF molecules (counter ion not illustrated). d) Crystal structure (20-Crown-6)T2:$KClO_4$ stabilized by one acetonitrile molecule and one perchlorate ion (solvent molecules and counter ion are faded).

To demonstrate reversibility, 15-Crown-5 was added at the end of the titration series and the initial absorption peak was restored. Similar to the analogous small molecules units, the extinction coefficient of the polymer decreased while the complex was formed. A low concentration of 50 µg mL^{-1} is used for the titration of **P1**. When $KBPh_4$ was added, no color change was observed (Figure 5b). Photoluminescence measurements with $NaBPh_4$ were carried out and the emission spectrum shifts 76 nm toward higher energy (Figure 5d).

Table 2 summarizes the responses of the polymers **P1–P4** as well as the small molecules toward sodium and potassium salts in THF. It was found that the sodium selective polymers **P1** and **P3** have the highest selectivity and only form the twisted complexes with sodium salts. **P2** and **P4** are selective toward potassium salts while **P4** also shows a 10 nm shift when 200 equivalents of sodium ions were added, which can be explained by interaction of the crown ether and the salt which does not twist the structure similar as found for the small molecule (20-Crown-6)T2 and sodium ions. More polar solvents such as DMF solubilize the alkali metal salts better and lower the complex stability constant by a factor of 1000 (Supporting Information).

2.5. DFT Calculations

We calculated the energy of the highest occupied molecular orbital (HOMO) of a molecule consisting of three BDT and two T2 units by using hybrid density functional theory (DFT) calculation in vacuum at B3LYP/6-31G(d) level of theory. The HOMOs



Scheme 3. Synthesis of polymers P1–P4.

© 2015 The Authors. Published by WILEY-VCH Verlag GmbH & Co. KGaA, Weinheim

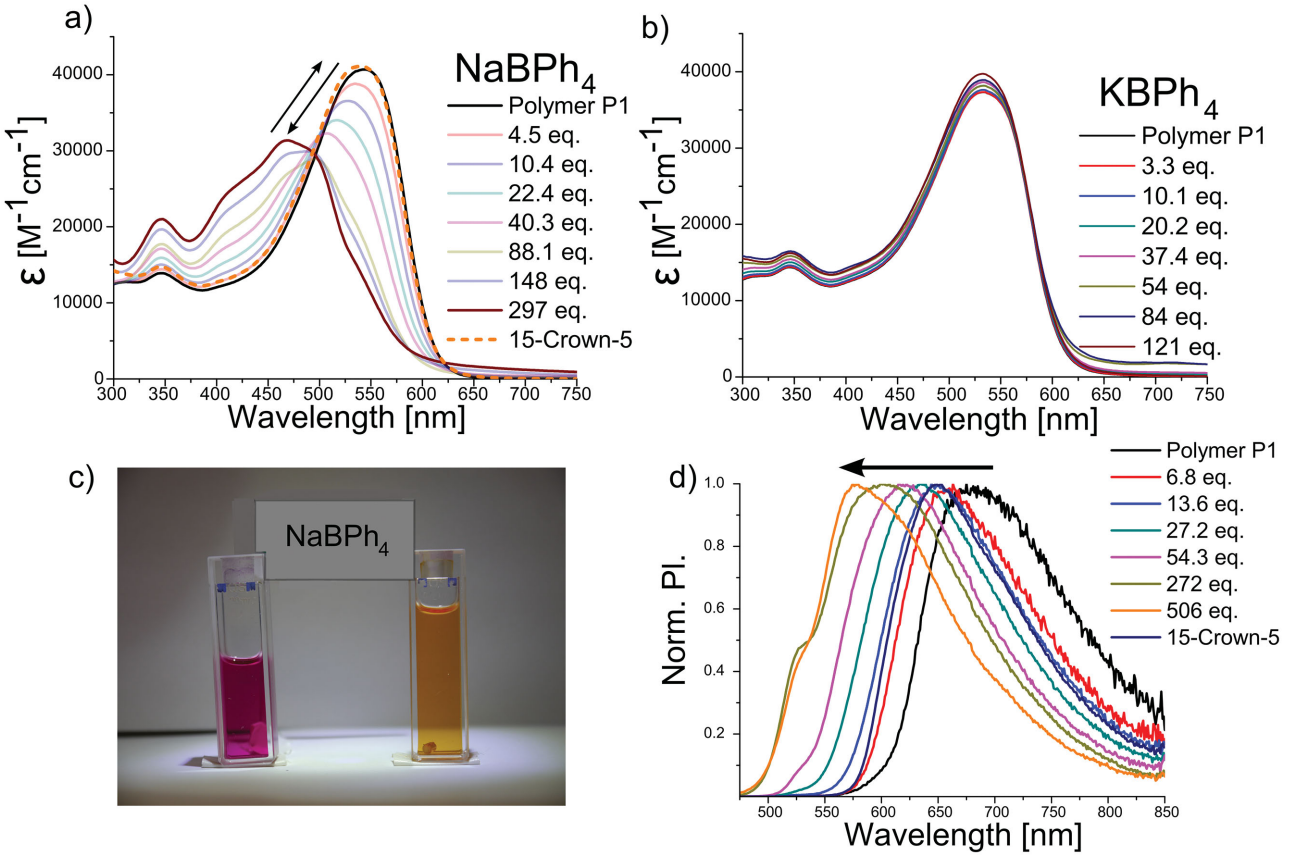


Figure 5. Titration experiments of P1 and $MBPh_4$ (M = Na, K) in THF, a) addition of $NaBPh_4$ and 15-Crown-5, b) addition of $KBPh_4$, c) color change after addition of 300 equivalents $NaBPh_4$, d) PL shift with $NaBPh_4$.

for the planar and for the twisted structure were calculated to be –4.59 and –5.06 eV, respectively. Calculations for the twisted structure were carried out starting from the data obtained from the crystal structure without the salt to use a simple level of DFT theory. The ionization potentials of **P3** with and without $NaClO_4$ were measured by photoelectron spectroscopy and the ionization potential increased from –4.8 to –5.6 eV when sodium salts were preloaded into the thin film.

The larger ionization potential obtained from the PESA measurements can be explained by a charge transfer from the ligand to the sodium ions which also affects the ionization potential of the polymer. **Figure 6** illustrates the spatial distributions of the HOMOs of the planar and twisted structure and shows the decrease in conjugation length when the structure is twisted.

Table 2. Optical responses of the polymers (P1–P4) and small molecules ((17-Crown-5)T2, (20-Crown-6)T2) toward $MBPh_4$ (M = Na, K) in THF.

	Absorption max. [nm]	Shift in UV–vis [nm]	Shift in PL [nm]
P1	542	75-Na	76-Na
P2	558	40-K	20-K
P3	510	54-Na	63-Na
P4	520	64-K	32-K
(17-Crown-5)T2	336	40-Na	–
(20-Crown-6)T2	339	50-K	–

2.6. Sensitivity Measurements

An optical sensor comprising a polymer rather than a small molecule has the advantage that the sensitivity is amplified by the number of conjugated repeat units containing the crown ether ligand along the backbone. **Figure 7**a,b shows the responses of small molecule (17-Crown-5)T2 and polymer **P3** toward $NaBPh_4$ in THF. It was observed that the absorption onset energy of the polymer already shifts at lower salt concentrations while the small molecule shows no change. This can be explained by considering that in the case of the polymer, each crown ether bithiophene is in conjugation with the BDT units along the backbone, and thus the effect of the alkali metal salts on absorption and extinction coefficient is cooperative and scales with the number of conjugated units. This means the higher the conjugation length of the crown ether polymers before the salt addition the higher will be the response signal and sensitivity. For a small molecule based sensor a higher concentration of salt is necessary to shift the reaction equilibrium to the twisted complex side.

Figure 7c presents the change of the extinction coefficient and absorption onset of polymer **P3** and small molecule

© 2015 The Authors. Published by WILEY-VCH Verlag GmbH & Co. KGaA, Weinheim

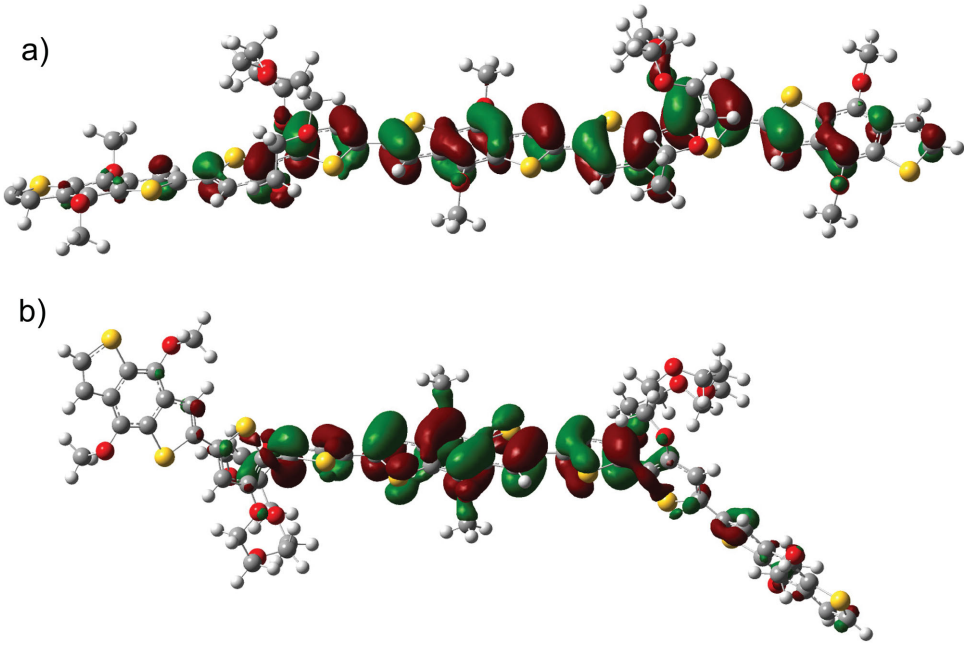


Figure 6. HOMO of the a) planar and b) twisted molecule with three BDT and two T2 units.

(17-Crown-5)T2 in solution when the concentration of sodium salt is increased (extinction coefficient of the absorption maximum and absorption onset as shown in Figure 7a,b related to the concentration of sodium salt in THF). When the change in extinction coefficient is the signal of choice (Figure 7c, black lines) it can be observed that the polymer has a higher sensitivity toward sodium ions at concentrations between 0.2×10^{-3} and 1.0×10^{-3} M than the small molecule. The peak sensitivity for the polymer **P3** is at a concentration of 0.4×10^{-3} M. The upper detection limit for sodium ions of polymer **P3** is reached at 1.0×10^{-3} M and at a concentration of 0.2×10^{-3} M the polymer has a two times larger sensitivity than the small molecule. Small molecule (17-Crown-5)T2 has a higher sensitivity at lower sodium-salt concentrations. When the absorption onset is the signal of choice (Figure 7c, blue lines) the polymer outperforms the small molecule and shows the advantage of an optical sensor based on a polymeric structure rather than a small molecule. The detection range of the ion selective polymers can be adjusted to the requirements of the desired application by the synthetic design of the polymer where the complex stability constant will determine the sensitivity range. For example, the detection of sodium ions in extracellular fluids requires a detection range with a peak sensitivity in the millimolar range (sodium concentration in extracellular fluid: 135×10^{-3}–145×10^{-3} M[27]). This can be achieved by a polymer structure based on a similar detector unit as (17-Crown-5)T2 and (20-Crown-6)T2 with a similar complex stability constant in aqueous solutions. To demonstrate that (17-Crown-5)T2 and polymer P3 retained their selectivity toward sodium ions in the presence of other alkali metal ions, titration experiments with a

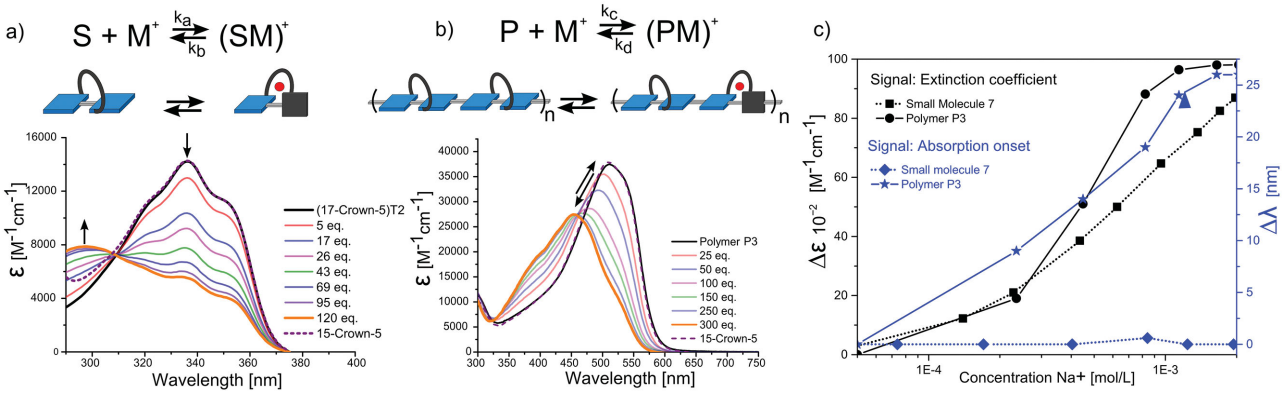


Figure 7. Comparison of a visible sensor based on a) small molecule and response of (17-Crown-5)T2 toward $NaBPh_4$ in THF, b) polymeric structure, and response of polymer P3 toward $NaBPh_4$ in THF, c) sensitivity measurements of small molecule (17-Crown-5)T2 and polymer P3. The *X*-axis shows the concentration of $NaBPh_4$ in THF. a) *Y*-axis left: difference in extinction coefficient ($\Delta\varepsilon = \varepsilon_0 - \varepsilon$). Right *Y*-axis: difference in absorption onset $\Delta\lambda = \lambda_0 - \lambda$).

© 2015 The Authors. Published by WILEY-VCH Verlag GmbH & Co. KGaA, Weinheim

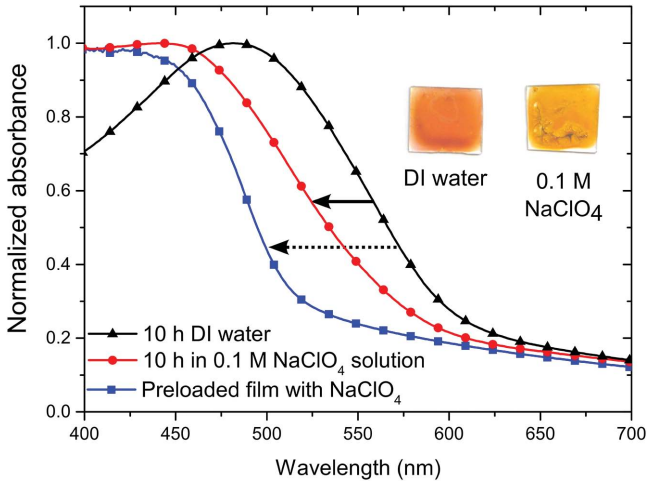


Figure 8. UV–vis spectroscopy of the optical solid state sensor. Thin films were immersed for 10 h in DI water (black line), 0.1 M $NaClO_4$ (red line), and preloaded with $NaClO_4$ (blue line) and dried at 100 °C.

background concentration of 1.0×10^{-3} M $KBPh_4$ were carried out and no decrease of selectivity was observed (Supporting Information).

2.7. Solid State Sensor

Finally, we were able to develop a visible solid state sensor for sodium ions. We prepared polymer–polymer blends with PVA and sodium selective polymer **P3** in a mass ratio of 20:1. Water-insolubility of the films was achieved by cross-linking the blend with maleic anhydride at 110 °C.[28] The films were then immersed in 0.1 M aqueous $NaClO_4$ solution and deionized (DI) water as a reference for 10 h. Hydrogel formation was observed in water (Supporting Information) and after 10 h the films were dried at 100 °C. A color change was already visually observed on comparison of the two films. UV-vis spectroscopy was carried out on the dried films and a 35 nm shift of the absorption maximum toward higher energy was observed as shown in **Figure 8** while a broad absorption peak between 350 and 450 nm was formed. A preloaded film with $NaClO_4$ was prepared under the same conditions to compare the shift of the absorption peak (blue line) and the result is similar to the absorption shift observed for the 0.1 M $NaClO_4$ solution. To demonstrate reversibility of the complex formation, the films were immersed in deionized water for 10 h and a shift toward the initial absorption peak was observed after drying the films.

3. Conclusion

In conclusion we successfully synthesized a series of crown ether bithiophene ion selective small molecules and polymers. The crown ether units only undergo a backbone twist when sodium or potassium ions are present where the selectivity depends on the size of the crown ether ring. We confirmed the structural backbone twist by UV–vis and NMR measurements as well as an X-ray diffraction study of single crystals. The selectivity of the crown ether is maintained after incorporating into a polymer structure where a shift of the absorption and fluorescence peak of up to 75 nm toward higher energy can be observed upon alkali ion complexation. We found that the sensitivity increases in a polymeric structure and outperforms an equivalent small molecule structure. Compared to other approaches[29] for selective alkali metal ion detection in solution, the presented optical sensor consists only of a one compound polymer system. The advantage of the optical sensor materials is that in addition to PL spectroscopy,[29,30] simple UV–vis spectroscopy can also be used to detect alkali metal ions in solution. The selectivity toward different alkali metal ions can be adjusted by varying the ring size of the crown ether ring and selectivity is also retrained in the background of other alkali metal ions. Finally, we were able to incorporate the sodium selective polymer into a PVA matrix to demonstrate the first example of a solid state optical sodium sensor based on conjugated polymers.

Supporting Information

Supporting Information is available from the Wiley Online Library or from the author.

Acknowledgements

We thank EPSRC Project EP/G037515/1, EC FP7 Project SC2 (610115), EC FP7 Project ArtESun (604397), and EC FP7 POLYMED (612538) for the financial support.

Received: September 7, 2015
Revised: October 29, 2015
Published online: December 16, 2015

[1] T. Hayashita, K. Kunogi, H. Yamamoto, S. Shinkai, *Anal. Sci.* **1997**, *13*, 161.
[2] E. Bakker, M. Lerchi, T. Rosatzin, B. Rusterholz, W. Wimon, *Anal. Chim. Acta* **1993**, *278*, 211.
[3] U. Oesch, D. Ammann, W. Simon, *Clin. Chem.* **1986**, *32*, 1448.
[4] X. Yang, K. Wang, C. Guo, *Anal. Chim. Acta* **2000**, *407*, 45.
[5] E. Wang, L. Zhu, L. Ma, H. Patel, *Anal. Chim. Acta* **1997**, *357*, 85.
[6] C. J. Pedersen, *J. Am. Chem. Soc.* **1967**, *89*, 2495.
[7] G. B. Levy, *Clin. Chem.* **1981**, *27*, 1435.
[8] G. J. Moody, B. B. Saad, J. D. Thomas, *Analyst* **1989**, *114*, 15.
[9] M. a. Arnold, *Clin. Chem.* **1991**, *37*, 1319.
[10] Y.-H. Kim, J.-I. Hong, *Chem. Commun.* **2002**, 512.
[11] O. Chemie, D. U. Wiirzburg, A. Hubland, **1995**, *129*, 124.
[12] T. Yamamoto, M. Omote, Y. Miyazaki, A. Kashiwazaki, B.-L. Lee, T. Kanbara, K. Osakada, T. Inoue, K. Kubota, *Macromolecules* **1997**, *30*, 7158.
[13] T. K. Tran, K. Smaali, M. Hardouin, Q. Bricaud, M. Oçafrain, P. Blanchard, S. Lenfant, S. Godey, J. Roncali, D. Vuillaume, *Adv. Mater.* **2013**, *25*, 427.
[14] A. I. Vedernikov, E. N. Ushakov, L. G. Kuz'mina, A. V. Churakov, Y. a. Strelenko, M. Wörner, A. M. Braun, J. a. K. Howard, M. V. Alfimov, S. P. Gromov, *J. Phys. Org. Chem.* **2010**, *23*, 195.

© 2015 The Authors. Published by WILEY-VCH Verlag GmbH & Co. KGaA, Weinheim

[15] M. J. Marsella, T. M. Swager, *J. Am. Chem. Soc.* **1993**, *115*, 12214.
[16] T. Oike, T. Kurata, K. Takimiya, T. Otsubo, Y. Aso, H. Zhang, Y. Araki, O. Ito, *J. Am. Chem. Soc.* **2005**, *127*, 15372.
[17] J. D. E. Chaffin, J. M. Barker, P. R. Huddleston, *J. Chem. Soc. Perkin Trans.* **2001**, *1*, 1398.
[18] K. Lu, J. Fang, X. Zhu, H. Yan, D. Li, C. Di, Y. Yang, Z. Wei, *New J. Chem.* **2013**, *37*, 1728.
[19] H.-J. Buschmann, *J. Solut. Chem.* **1988**, *17*, 277.
[20] R. D. Boss, A. I. Popov, *Inorg. Chem.* **1986**, *25*, 1747.
[21] S. Fery-Forgues, M. T. Le Bris, J. P. Guette, B. Valeur, *J. Phys. Chem.* **1988**, *92*, 6233.
[22] M. B. Gholivand, M. Shamsipur, *Inorganica Chim. Acta* **1986**, *121*, 53.
[23] N. Hergue, P. Leriche, P. Blanchard, M. Allain, N. Gallego-Planas, P. Frere, J. Roncali, *New J. Chem.* **2008**, *32*, 932.
[24] J.-C. Chen, H.-C. Wu, C.-J. Chiang, L.-C. Peng, T. Chen, L. Xing, S.-W. Liu, *Polymer (Guildf)*. **2011**, *52*, 6011.
[25] L. Biniek, B. C. Schroeder, J. E. Donaghey, N. Yaacobi-Gross, R. S. Ashraf, Y. W. Soon, C. B. Nielsen, J. R. Durrant, T. D. Anthopoulos, I. McCulloch, *Macromolecules* **2013**, *46*, 727.
[26] P. Liu, K. Zhang, F. Liu, Y. Jin, S. Liu, T. P. Russell, H.-L. Yip, F. Huang, Y. Cao, *Chem. Mater.* **2014**, *26*, 3009.
[27] M. G. Bianchetti, G. D. Simonetti, A. Bettinelli, *Ital. J. Pediatr.* **2009**, *35*, 36.
[28] J. M. Gohil, A. Bhattacharya, P. Ray, *J. Polym. Res.* **2006**, *13*, 161.
[29] B. L. Nguyen, J.-E. Jeong, I. H. Jung, B. Kim, V. S. Le, I. Kim, K. Kyhm, H. Y. Woo, *Adv. Funct. Mater.* **2014**, *24*, 1748.
[30] B. Sui, X. Yue, B. Kim, K. D. Belfield, *ACS Appl. Mater. Interfaces* **2015**, *7*, 17565.

© 2015 The Authors. Published by WILEY-VCH Verlag GmbH & Co. KGaA, Weinheim